A Study in Monte Carlo Simulation of Modified DLA

K. -C. Chiu, F. -S. Lee, S. -J. Tu, S. -M. Young, W. -Y. Hsu, C. -F. Chen, C. -S. Ro

Department of Physics, Chung-Yuan Christian University, Chung-Li, Taiwan 32023, R.O.C.

(Received September 27, 1991; revised manuscript received December 20, 1991)

A Monte Carlo simulation of modified diffusion-limited aggregation (DLA) is applied to study the morphological evolution of pattern formation. *In* this modified DLA simulation, the sticking coefficient and the mean-field parameter are varied to simulate the physical properties of the system and the nature of the processes. By tuning these two parameters, a rich variety of pattern formation observed in many physical processes due to spatial and temporal fluctuations can be reconstructed from this simple method.

I. INTRODUCTION

Recently, there has been a growing interest about the non-equilibrium growth phenomena in various fields of science and technology, such as morphological evolution of growing crystals[1-6] and cluster-cluster aggregation,[7-12] tip splitting of viscous fingers in a Hele-Shaw cell,[13-15] and pattern of dielectric breakdown.[16] For all of these systems, if diffusion is the rate-limited step of the growth process, then the field parameter (such as concentration, pressure, or electrostatic potential) satisfies a diffusion equation. Hence, the diffusion-limited aggregation (DLA) model, which studies the diffusion equation with inclusion of spatial and temporal fluctuations, is believed to be the underlying physical mechanism responsible for the observed fractal pattern.

The DLA model can be studied by a Monte Carlo method in a discretized version.[1,7-10] In Monte Carlo simulation of the standard DLA model, an initial cluster is represented by putting a seed particle at the center of the domain. Another particle is randomly introduced from a distant boundary. After many random walks, it comes to one of the nearest neighbor sites of the cluster and sticks there to become part of the cluster. The cluster grows as the procedure is repeated.

In order to make DLA model to be more realistic to the physical situation, several modifications were made. The first one was made by considering the non-unity sticking probability, i.e., after encounter the cluster the random walking particle can only have a certain probability to be stuck. This sitcking probability is a function of number of nearest neighbors[12] (one parameter DLA model), and is given as

$$P_i = S^{3-n_i} \tag{1}$$

where S is the sticking coefficient ($S \leq 1$) and n_i is the number of occupied nearest neighbors at the i^{th} site. In this case, the simulation can be related to the local generalized field intensity (such as concentration gradient, electric field[16] etc.). Another modification was made by considering the mean-field effect which is also called the average scheme.[13,15,17] In this average scheme, if the condition (e.g., determined by eq(1)) on a specific i^{th} site around the cluster is allowed for a random walk particle to be stuck, it does not immediately occupy that site. Instead of being occupied, this i^{th} site is only registered by being visited once. Then, the procedure is repeated until the registration number of being visited for an unoccupied i^{th} site exceeds a certain mean-field parameter, M, this site becomes occupied. For M = 1, this corresponds a standard DLA model. For M approachs infinity, it should be corresponding to the solution of continuum diffusion equation with moving boundary conditions.

The theoretical analysis of the morphological evolution during pattern formation can be understood from the Mullins-Sekerka instability' * which takes place whenever one part of the interface protrudes locally faster than the surrounding region. By using perturbation theory, the interface instability condition can be determined from a dispersion relation.[4,5,7,18] However, in order to predict the time evolution of pattern formation, numerical methods are usually required.

In this paper, we present our results from a study of this modified DLA model with two variable parameters (sticking coefficient and mean-field parameter). By tuning these two parameters to simulate the spatial and temporal fluctuation, the physical significance and the relation to pattern formation observed in many physical processes are discussed.

II. SIMULATION PROCEDURE

The fundamental feature of the simulation procedure is similar to those in modified DLA models with average scheme.[1,15] A 400 x 400 square lattice with a seed particle at the origin was chosen. In order to save computer time, two processes are adopted. First, instead of introducing from a very distant boundary, the particles are randomly start from a circular perimeter with large enough radius R_{in}. Second, after many random walks, the particle can have the opportunity to walk back. Once it exceeds a circular perimeter with radius R_{out} ($> R_{in}$), it is disregarded. The circular boundary conditions are chosen in order to avoid the flux increase artificially in diagonal direction and the difference of diffusive distance in the axial and diagonal direction which are imposed by the square boundary conditions. The random walk particle moves with one grid length at each step on the 2D square lattice. After encounter the cluster, the sticking probability is determined by eq. (1). The non-sticking particle is allowed to diffuse to one of the available sites (bulk site or interface site) with equal opportunity. The bulk site is a lattice site without any nearest neighbor, and the interface site is a site at least with one nearest neighbor. The average scheme is incorporated through the variable mean-field

parameter M from 1 to 50. The flowchart of this simulation procedure is shown in Fig. 1. To reduce the correlation of each random process, the same four random number generators (RAN2 function") are used independently for the processes for introducing particle from circular perimeter, random walking, determing the stickiness, and jumping to one of the available sites for non-sticking particle. To obtain a better random distribution, all the random number generaters are re-shuffling after every 3000 growth units being aggregated within the cluster.

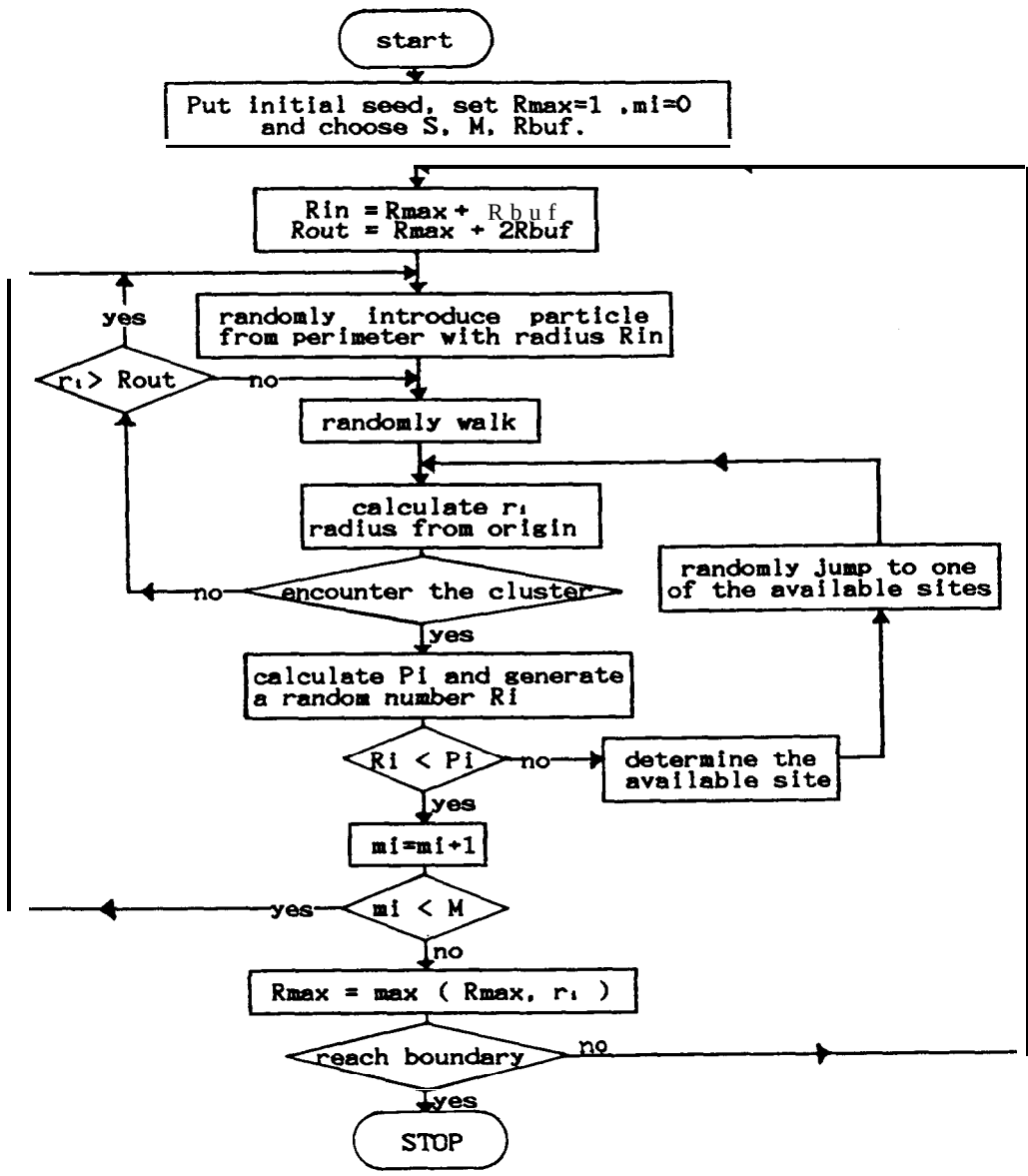

FIG. 1. Flowchart of simulation procedure.

III. RESULTS AND DISCUSSION

III-1. Comparison with a standard **DLA** model (**S** = 1, M = 1)

Before addressing any further details from modified DLA models, we will start with a standard DLA model (S = 1, M = 1). From the earlier published results of standard DLA model, some of them shown a strong anisotropic behavior in global scale. But in reality, most of the pattern for individual cluster aggregation without coupling in between usually exhibit certain degree of symmetric or isotropic shape to reflect the uniformly random diffusion through the bulk[4,6,20] unless the boundary is specified nonuniformly.[14] Therefore, for the simulation of a single cluster aggregation, the initially starting perimeter should lie on one of the equipotential curves (or equal concentration curves). As schematically shown in Fig. 2 for 2D isotropic boundary condition, near the region of the growing cluster, the equipotential curves vary strongly with the shape of the cluster for the cases both without and with the shift in the center of mass (CM). Only at region enough far-away from the cluster, the equipotential curve may look like a circle (or related to the imposed boundary shape). Hence, we choose circular boundary conditions with $R_{in} = R_{max} + R_{buf}$ and $R_{out} = R_{max} + 2*R_{buf}$, where R_{max} is the largest radius of the as-grown cluster, R_{buf} is the width for the inner or outer buffer annulus for diffusion process to be taken. The influence on the fractal pattern for different values of R_{buf} is shown in Fig. 3. During the growth process, once there is any protrudent spot due to local spatial fluctuation, the local gradient of potential is increased dramatically. If the initially introducing particle is still from a circle with a small R_{in}, i.e. $R_{buf} = R_{buf0} = 30$ is a small constant. Then this

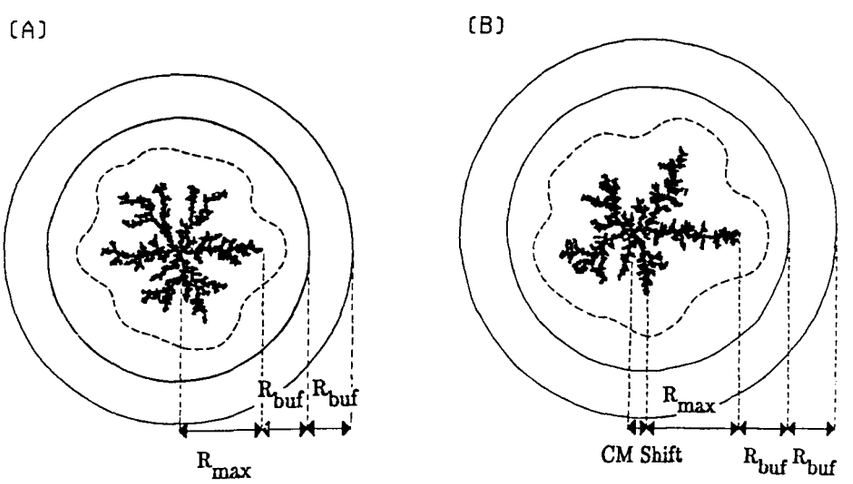

FIG. 2. Schematic diagram of equipotential (concentration) curves (A) without (B) with shift in CM around the cluster.

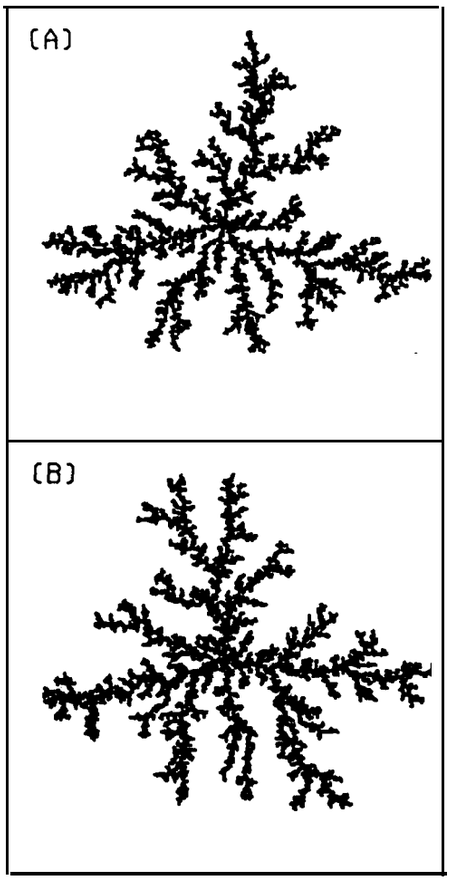

FIG. 3. Fractal patterns correspond to different choice of R_{buf} (A) $R_{buf0} = 30$, and (B) $R_{buf1} = 0.5\,R_{max} + 30$.

circle is not a good equipotential curve after the cluster growing to be a larger size. Thus, we end up with an artificial increment of particle flux (or electric flux) near the protrudent spot and hence an asymmetric pattern as shown in Fig. 3(A) is obtained. For $R_{buf} = R_{buf1} = 0.5*R_{max} + 30$, which the width of the diffusive buffering annulus increases with respect to the growth of the cluster, sufficient bulk diffusion process takes place inside this buffer and more isotropic behavior is expected as shown in Fig. 3(B). This small variance in fractal pattern with respect to the change in R_{in} and R_{out} was also reported by Luo et al., [11] recently. From their results, this small variance, though is negligible in square boundary, but still can be noted in circular boundary with R_{in} from $R_{max} + 6$ to $R_{max} + 24$. As mentioned above, the circle with sufficient large R_{in} can resemble to one of the equipotential curves, hence,

with the result from Fig. 3(B), $R_{in} = R_{max} + R_{buf1}$ is chosen from hereafter as a compromise between the saving of computer effort and the resemblance of equipotential curves.

When the initial seed starts to grow, the center of mass (CM) for the growing cluster may not coincide with the origin, as shown in Fig. 2(B). In this case, the protrudent branch changes the potential curve. Hence, a circular perimeter based on the fixed origin as a center is not a good equipotential curve anymore unless R_{in} is very large. However, due to the computational limits, R_{in} usually is not chosen very large. The correction of the shift of CM is necessary especially for the individual nucleation within a homogeneous fluid. Thus, once a particle is stuck and is become part of the cluster, the CM of the as-grown cluster is re-calculated. The following

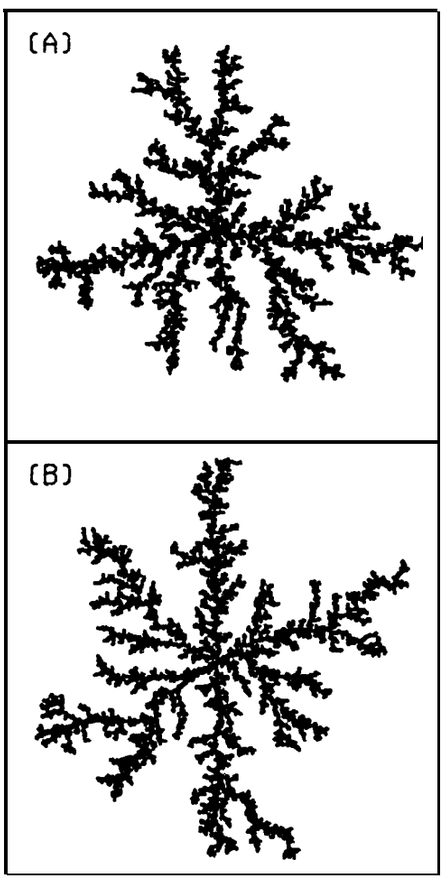

FIG. 4. Fractal patterns correspond to R_{buf1} and (A) without (B) with CM correction.

particle is then introduced from a circle with R_{in} based on this new CM. Figure 4 shows the effect of CM correction on the fractal pattern. One can see that with CM correction the cluster exhibits a reasonable isotropic behavior corresponding to the spherically symmetric diffusion field.[22] In our simulation, the shift of CM during growth process is, in general, less than 10 lattice grids.

The fractal dimension D for a cluster can be defined by the expression,[7]

$$N(r_g) \approx r_g^D, \tag{2}$$

where r_g is the radius of gyration for the cluster and $N(r_g)$ is the total number of particles within that cluster. For example, a cluster as shown in Fig. 4(B), during the growth process with N = 3000, 6000, 9000, and 9964, the radii of gyration are calculated, respectively. Then, from the plot for $\log_{10}N(r_g)$ vs. $\log_{10}r_g$ as shown in Fig. 5(A), one can obtain the fractal dimension. In addition, an alternative method to determine the fractal dimension can also be defined by[7]

$$N(R) \approx R^D, \tag{3}$$

where R is the distance from CM, and N(R) is the number of particles within a circle of radius R. From the slope of $\log_{10}N(R)$ vs. $\log_{10}R$, as shown in Fig. 5(B), D can be determined. It is interesting to note that the slope is not a good constant in the whole region. Only in the region for R greater than twice of maximum CM shift (to avoid the singularity at CM) and less than half of R_{max} (to obtain fully developed cluster), the slope is determined to represent the nearly fully developed cluster. By using eqs. (2) and (3), and from an average of three different clusters, the mean fractal dimension D for standard DLA clusters obtained by this work is 1.62 $\pm$ 0.02, where the error refers the average deviation. In principle, the results obtained from eqs. (2) and (3) should be identical for fully developed cluster. From a comparison with other theoretical predictions[23,24] and numerical simulations[7-9,12,21,25] in 2D square lattice as listed in Table I, the result obtained by this work is smaller. This difference can be understood by non-fully developed character in view of the developing behavior from Fig. 5(B). In order to obtain more accurate results, simulation in larger cluster is necessary.

III-2. Effects of the variable sticking coefficient

If the sticking probability is less than 1, the impinging particle (or, in general, spatial fluctuation) has a chance to continue its diffusion process either near the interface or back to the bulk region. The magnitude of S in eq. (1) depends on the physical properties of the system, such as temperature, bond strength, and /or interfacial tension, etc., and can be derived from the equilibrium thermodynamics. The surface kinetics in this model is simply (in the first order sense) included by counting the relative numbers of bulk site with respect to interface site. If there is more available interface sites than bulk sites, then surface diffusion is dominant. Otherwise, evaporation is dominant (e.g., the tip of each branch). Therefore, as shown in Fig. 6 for

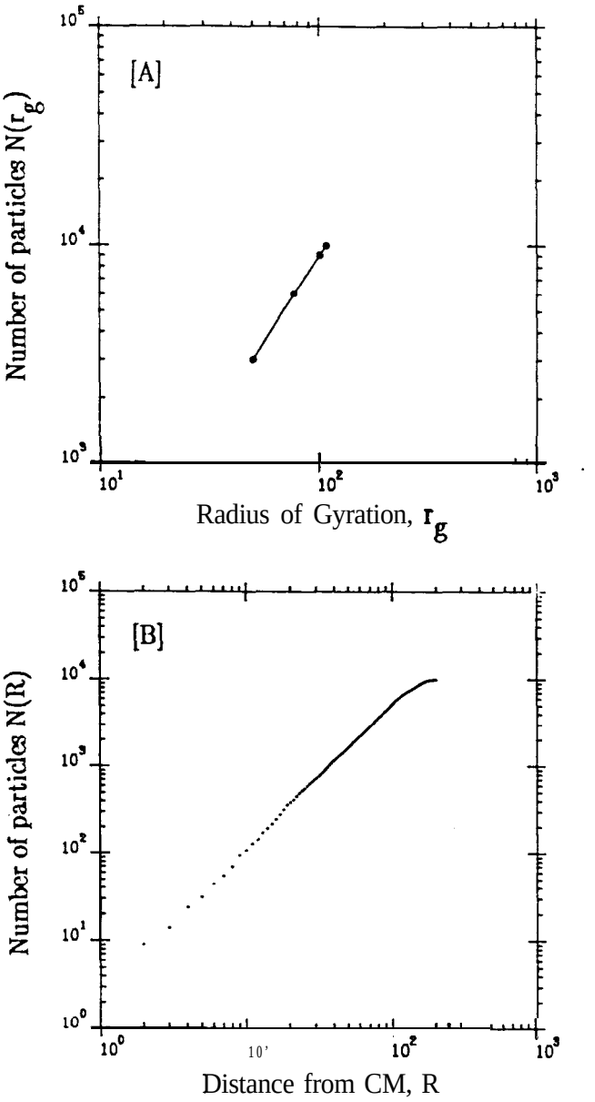

FIG. 5. (A) Plot of $\log_{10}N(r_g)$ vs. $\log_{10}r_g$ from eq. (2), and (B) plot of $\log_{10}N(R)$ vs. $\log_{10}R$ from eq. (3), for a standard DLA cluster as shown in Fig. 4(B).

a DLA model with M = 1, the cluster looks more compact as S decreasing from 1 to 0.3. The simulation with smaller value of S refers to the system with less surface adsorption or weaker bond strength, and hence represents a system with less influence by the spatial fluctuation. Besides, we have noted that the shift of CM is less for cluster with small S. If the fractal behavior is assumed to follow eqs. (2) and (3) and from an average of different clusters as listed in Table

TABLE I. Comparison of D with other works for 2D square lattice

	D
Theoretical prediction:	
Turkevich and Scher[23]	1.67
Muthukumar[24]	1.67
Numerical simulation:	
Vicsek[7]	1.70 ± 0.06
Witten and Sander[8,9]	1.66 ± 0.04
Banavar et al[12]	1.72 ± 0.08
Luo et al[21]	1.67 ± 0.03
Meakin[25]	1.66 ± 0.01
This work	1.62 ± 0.02

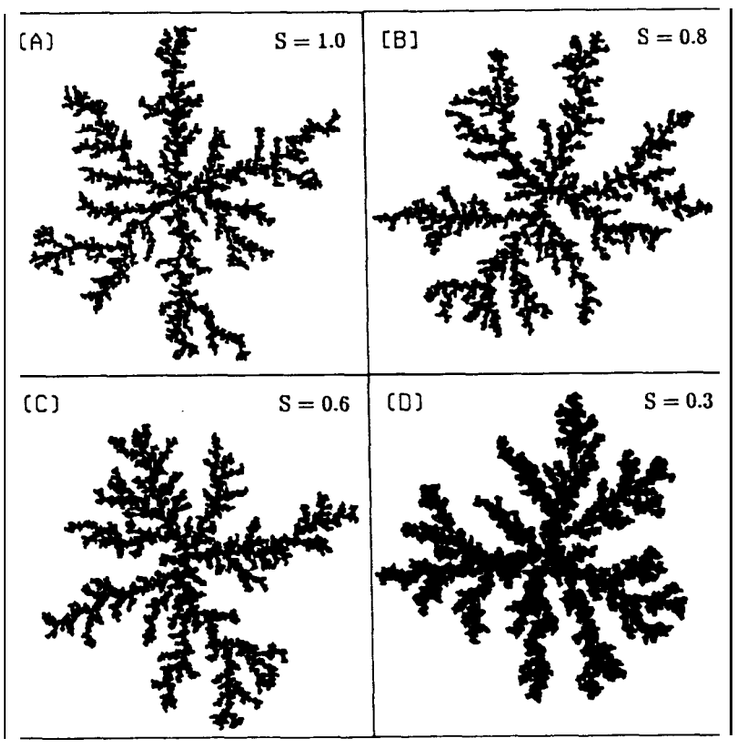

FIG. 6. Fractal patterns of modified DLA models (M = 1) with varying sticking coefficient (A) S = 1.0, (B) S = 0.8, (C) S = 0.6, (D) S = 0.3.

II, the mean fractal dimension D increases with decreasing S. These results are qualitatively in agreement with those obtained by Banavar, et al.[12]

TABLE II. Relations between S and D (with M = 1)

S	cluster size	mean value of D
1.0	10000	1.62 ± 0.02
0.8	11000	1.64 ± 0.06
0.6	13000	1.66 ± 0.04
0.3	22600	1.71 ± 0.03

In addition, Niemeyer et al[16] had studied the functional dependence of the sticking probability with respect to the local field. They found that the fractal dimension increases for the weaker functional dependence. Recently, from a derivation of kinetic theory, Xiao et al,[1-3] proposed that the sticking probability is a sophisticated function (other than eq.(l)) of supersaturation, temperature, and bond strength. In that modified DLA model, second nearest neighbor interaction, effects from mean free path and external drift, etc., had been included to make the modified DLA model more versatile. A study about this sophisticated model and its applications to vapor growth system is undergoing in our group.

III-3. Effects of the mean-field parameter M

By applying the average scheme to DLA models, several workers[13,15,17] usually paid their attention to the dramatic effects in noise reduction of the growing cluster. We would like to emphasize the fundamental physical significance associated to the mean-field parameter. From the thermodynamic point of view, it is well known that the quasistatic growth process closely approximates a succession of equilibrium states. In reality, the growth process or pattern formation process usually takes place in a certain degree far from the quasistatic process. By tuning the value of M, one can simulate different degrees of non-equilibrium during the growth process, such as finite pulling rate or cooling rate. Figure 7 shows the modified DLA results with S = 1.0 and for variable values of M = 2, 5, 10, and 50. Together with Fig. 6(A) for M = 1, one see that the structure patterns change from isotropic fractal → dendrite → anisotropic needle. For small M, it corresponds to a far-from-equilibrium growth process. The structure looks like the results obtained from suddenly frozen growth process which does not have enough time to reflect the underlying lattice shape and results in an isotropic fractal. For large M, it corresponds to a nearly quasistatic process and represents a system insensitive to temporal fluctuations (shot noise). Due to the 2D square grid used and the solid-on-solid growth condition (with nearest-neighbor interaction only) imposed during the simulation process, the four major fingers (with anisotropic cross-like shape for the cases with larger M) are resulted from the

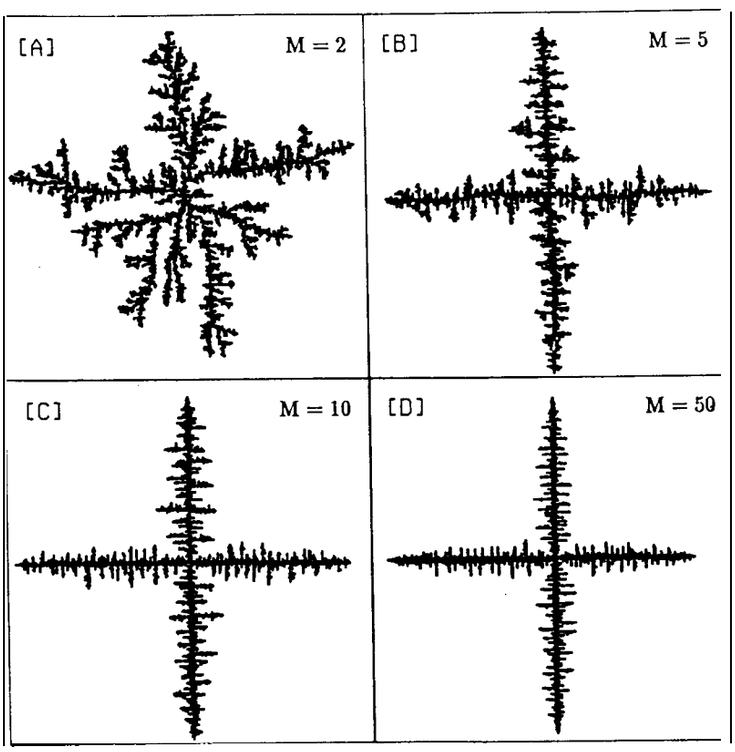

FIG. 7. Fractal patterns of **modified** DLA models (S = 1.0) with variable average scheme parameter (A) M = 2, (B) M = 5, (C) M = 10, (D) M = 50.

growth along the "easy" direction through Mullins-Sekerka instability.[18,26] Again, if fractal behavior follows eqs. (2) and (3), and from an average over different clusters, the variation for the mean fractal dimension D with respect to the variable values of M are listed in Table III.

It was argued that the average scheme can be used to reveal the asymptotic behavior of

TABLE III. Relations between M and D (with S = 1)

M	cluster size	mean value of D
1	10000	1.62 ± 0.02
2	8600	1.62 ± 0.05
5	5300	1.34 ± 0.05
10	5000	1.29 ± 0.06
50	4100	1.19 ± 0.07

DLA cluster using considerably smaller number of particles.[7] However, we believe that the value of M has its physical meaning as mentioned above. Once we choose a specific value of M corresponding to the nature of the process, a fractal dimension associated to this cluster will be determined. For standard DLA in large scale simulation, if the value of R_{in} is not chosen large enough as comparing with the growing value of R_{max}, due to the artificial increment effect as shown in Fig. 2, a cluster with larger R_{max} may exhibit the cross-like shape as those obtained from modified DLA with large M. Even though these structures may look some what similar, but they are corresponding to different growth conditions.

IV. SUMMARY

The Monte Carlo simulation for a standard DLA model and modified DLA models with either variable sticking coefficient S or variable mean-field parameter M are studied. For a standard DLA model, the influence on the fractal pattern from the choice of R_{buf} and the CM correction are shown. It is believed that the CM correction can save a lot of computational effort. From modified DLA models with either variable S or variable M, the effects on the fractal pattern as well as fractal dimension are given. For a simulation with smaller S, it is less sensitive to spatial fluctuation and a compact pattern is obtained. For a simulation with very large M, it is closely approximated to a quasi-static process. For a strong non-quasistatic process, M should be set to a small value. Hence, by tuning the value of M, one can simulate the various degree of non-equilibrium processes.

ACKNOWLEDGMENT

This work is supported by National Science Council of the Republic of China under Grants NSC78-0208-M033-20 and NSC79-0208-M033-24. The help from the Computer Center of Ministry of Education of the Republic of China is acknowledged.

REFERENCES

1. R. -F. Xiao, J.I.D. Alexander, and F. Rosenberger, Phys. Rev. **A 38**, 2447 (1988).
2. R. -F. Xiao, J.I.D. Alexander, and F. Rosenberger, Phys. Rev. **A 39**, 6397 (1989).
3. R. -F. Xiao, J.I.D. Alexander, and F. Rosenberger, J. Crystal Growth **109**, 43 (1991).
4. J. S. Langer, Rev. Mod. Phys. 52, 1 (1980).
5. L. N. Brush, and R. F. Sekerka, J. Crystal Growth 96,419 (1989).
6. E. Ben-Jacob, and P. Garik, Nature 343,523 (1990).
7. T. Vicsek, *Fractal Growth Phenomena,* (World Scientific, Singapore 1989).
8. T. A. Witten, and L. M. Sander, Phys. Rev. Lett. **47**, 1400 (1981).
9. T. A. Witten, and L. M. Sander, Phys. Rev. **B 27**, 5686 (1983).

10. T. Vicsek, Phys. Rev. Lett. **53**, 2281 (1984).
11. T. Vicsek, Phys. Rev. A **32**, 3084 (1985).
12. J. R. Banavar, M. Kohmoto, and J. Roberts, Phys. Rev. A **33**, 2065 (1986).
13. J. Nittmann, and H. E. Stanley, Nature 321,663 (1986).
14. J. Nittmann, G. Daccord, and H. E. Stanley, Nature **314**, 141 (1985).
15. C. Tang, Phys. Rev **A 31**, 1977 (1985).
16. L. Niemeyer, L. Pietronero, and H. J. Wiesmann, Phys. Rev. Lett. **52**, 1033 (1984).
17. J. Kertesz, and T. Vicsek, J. Phys. A: Math. Gen. 19, L257 (1986).
18. W. W. Mullins, and R. F. Sekerka, J. Appl. Phys. 35,444 (1964).
19. W. H. Press, B. P. Flannery, S. A. Teukolsky, and W. T. Vetterling, ***Numerical Recipes: The Art of Scientific Computing*** (Cambridge University Press, London, 1986).
20. W. A Bentley, and W. J. Humphreys, Snow *Crystals* (Dover, New York, 1962).
21. Y.-L. Luo, W.-L. Yang, and S.-L. Lee, Bull. Inst. Chem. Academia Sinica (ROC) **38**, 65 (1991).
22. F. Family, T. Vicsek, and P. Meakin, Phys. Rev. Lett. 55,641 (1985).
23. L. A. Turkevich, and H. Scher, Phys. Rev. Lett. **55**, 1026 (1985).
24. M. Muthukumar, Phys. Rev. Lett. 50,839 (1983).
25. P. Meakm, Phys. Rev. A **33**, 3371 (1986).
26. R. C. Ball, Physica A **140**, 62 (1986).